TIME-RESOLVED FLUORESCENCE POLARIZATION FROM ORDERED BIOLOGICAL ASSEMBLIES

THOMAS P. BURGHARDT
Cardiovascular Research Institute, University of California at San Francisco, San Francisco, California 94143

ABSTRACT We calculate the time dependence of the polarized fluorescence signal from fluorescent-labeled elements of a biological assembly that are rotationally diffusing in an arbitrary three-dimensional angular potential. We have formulated this calculation using the model-independent description of the angular potential wherein the angular potential is described by an expansion in a complete set of orthonormal functions with the expansion coefficients (or order parameters) determined by time-independent methods (Burghardt, T. P., 1984, *Biopolymers*, 23:2382–2406). We have applied the calculation to fluorescent-labeled myosin cross-bridges in relaxed muscle fibers. In a related paper we describe the experimental observation of the myosin cross-bridges rotationally diffusing in an angular potential (Burghardt, T. P., and N. L. Thompson, 1985, *Biochemistry*, 24:3731–3735).

INTRODUCTION

Time-resolved fluorescence anisotropy decay after excitation by polarized light (TRFAD) is a technique employed in the study of the rotational diffusion of macromolecules in solution (1–6). Recently this technique has also been applied to the study of the rotational motion of elements of ordered systems such as the macromolecular constituents of biological assemblies; e.g., subfragment 1 (S-1) of skeletal muscle myofibrils (7) and proteins or lipids in lipid membranes (8–12). The rotational motion of free, rigid macromolecules is usually described by a model that assumes the macromolecule is a rigid body that freely diffuses about its principal hydrodynamic axes (1, 2, 13). When the equilibrium orientations of an isotropic ensemble of the macromolecules is perturbed, the relaxation back to equilibrium is characterized by an exponential decay. This behavior has been observed for some proteins in solution using TRFAD (3).

The mathematical description of motion of the constituents of ordered biological assemblies usually employs the model of rotational diffusion of the constituents in an angular potential. This model, often called restricted rotational diffusion, similarly predicts exponential relaxation to equilibrium in agreement with experiment (7, 8, 14–16). Aside from this feature, however, the modeling of restricted rotational diffusion differs from the free diffusion case in that the model really corresponds to many distinguishable models since there is ambiguity in assigning the form of the potential. In general, the exact form of the potential is not known a priori and a variety of potentials are equally suitable (8, 15). Experimental measurements with fluorescence, at present, are also not capable of distinguishing different potentials.

Ambiguity in the experimental determination of the time-independent angular distribution of constituent macromolecules in biological assemblies (a quantity directly related to the potential [17]) has led us in the past to develop model-independent methods to experimentally measure the angular distribution without specifying a model (18–21). Here we formulate a similar approach to the time-dependent problem and reduce the model dependence of the mathematical description by eliminating the model for the angular potential. The constituent macromolecules are still assumed to be rotationally diffusing in a potential, but the potential is described by an expansion in an appropriate complete set of orthonormal functions. The solution to the restricted rotational diffusion equation is also expressed as an expansion in the same orthonormal functions. When this solution, which is the probability density of molecular orientations, is used to calculate the time-dependent anisotropy decay, $r(t)$ we find it is an infinite sum of exponentials with relaxation times and amplitude factors that depend in a complicated manner on the diffusion constants and the expansion coefficients of the potential. This procedure uses the potential as expanded in orthonormal functions as it is measured with time-independent experiments when the model-independent forms of these techniques are used. As in previous model-independent treatments any explicit model of the potential can also be readily used in the formalism.

We derive a form of $r(t)$ that is applicable to a rigid macromolecule undergoing general restricted rotational diffusion by expressing $r(t)$ in terms of the eigenvalues and eigenvectors of the restricted rotational diffusion equation. The eigenvalues and eigenvectors depend on rotational diffusion constants and the expansion coefficients of the potential. This formula for $r(t)$, the time-independent

measurement of the potential, and the eigenvector solution to the restricted rotational diffusion equation specify the explicit time course of $r(t)$.

The application described in this paper calculates $r(t)$ for the restricted macromolecules in the assembly when the potential depends on two angular dimensions corresponding to Euler angles β and γ, see Fig. 1. This calculated $r(t)$ is used in a related paper to describe the rotational motion of myosin cross-bridges in relaxed muscle fibers (22).

The advantages of this analytical method over previous methods are (*a*) generality of application; (*b*) clarity in assigning features of the observed signal to physical features of the potential; and (*c*) ability to establish the theoretical limitations of the TRFAD technique for determining physical parameters of the system. These advantages are consequences of our method of solution wherein the time-dependent orientation probability density and the angular potential are expressed as sums of orthogonal functions.

THEORY

Equation of Motion

A macromolecule rotationally diffusing in a potential, with rotational diffusion constant D_i and rotational mobility u_i, is described by the operator equation

$$\frac{\partial P}{\partial t}(\Omega, t) = \sum_{i=1}^{3} \{D_i L_i^2 + u_i L_i (L_i V)\} P(\Omega, t) \equiv \mathcal{H}\, P(\Omega, t), \quad (1)$$

where Ω represents the three Euler angles α, β, and γ describing the orientation of a rigid body in space (see Fig. 1), t is time, $\mathcal{H}$ is a differential operator, and $P(\Omega, t)$ is the probability density for molecular orientations. The operators L_i are identical to the quantum mechanical orbital angular momentum operators and V is the angular potential. The equilibrium solution to Eq. 1, P_0, is given by $P_0 = c \exp(-V/kT)$, where c is a normalization constant, k is Boltzmann's constant, and T is the absolute temperature (17).

Operator $\mathcal{H}$ is not self-adjoint. To convert $\mathcal{H}$ to the self-adjoint form, H, we substitute $P(\Omega, t) = P_0^{1/2} Q(\Omega, t)$ into Eq. 1 and find

$$\frac{\partial Q}{\partial t}(\Omega, t) = P_0^{-1/2}\, \mathcal{H}\, P_0^{1/2}\quad Q(\Omega, t). \quad (2)$$

It can then be shown that

$$H = P_0^{-1/2}\, \mathcal{H}\, P_0^{1/2} = \sum_{i=1}^{3} D_i \{L_i^2 - (L_i \mathscr{f})^2 + (L_i^2 \mathscr{f})\} \quad (3)$$

when Einstein's relation $u_i = D_i/kT$ holds (23), and when $\mathscr{f} = V/2kT$ such that

$$P_0 = c \exp(-2\mathscr{f}). \quad (4)$$

Eq. 2 is the Sturm-Liouville problem and its solution is

$$Q(\Omega, t) = \sum_i a_i \varphi_i(\Omega) \exp(-E_i t), \quad (5)$$

where E_i are eigenvalues of the eigenvectors $\varphi_i(\Omega)$ and coefficients a_i are determined by an initial condition on $Q(\Omega, t)$. We expand both $\varphi_i(\Omega)$ and $\mathscr{f}$ in terms of the complete set of orthogonal functions, the Wigner rotation matrix elements (24), such that

$$\varphi_i(\Omega) = \sum_{\substack{\ell,m \\ n}} q^i_{\ell,m,n} \left(\frac{2\ell+1}{8\pi^2}\right)^{1/2} D^{\ell}_{m,n}(\Omega) \quad (6)$$

$$\mathscr{f}(\Omega) = \sum_{\substack{\ell,m \\ n}} f_{\ell,m,n} \left(\frac{2\ell+1}{8\pi^2}\right)^{1/2} D^{\ell}_{m,n}(\Omega). \quad (7)$$

The coefficients $f_{\ell,m,n}$ are determined from P_0 in Eq. 4 using the orthogonality relation for the $D^{\ell}_{m,n}$'s given by

$$\int_{\Omega_0} d\Omega\, D^{*\ell'}_{m',n'}(\Omega)\, D^{\ell}_{m,n}(\Omega) = \frac{8\pi^2}{2\ell+1} \delta_{\ell',\ell} \delta_{m',m} \delta_{n',n}, \quad (8)$$

where Ω_0 is the domain $0 \le \alpha \le 2\pi$, $0 \le \beta \le \pi$, $0 \le \gamma \le 2\pi$, and $\delta_{i,j}$ is the Kronecker delta. The eigenvalues E_i and coefficients $q^i_{\ell,m,n}$ are calculated from diagonalization of the matrix with elements $\langle j', h', k' | H | j, h, k \rangle$ where

$$\langle \Omega | j, h, k \rangle = \left(\frac{2j+1}{8\pi^2}\right)^{1/2} D^{j}_{h,k}(\Omega). \quad (9)$$

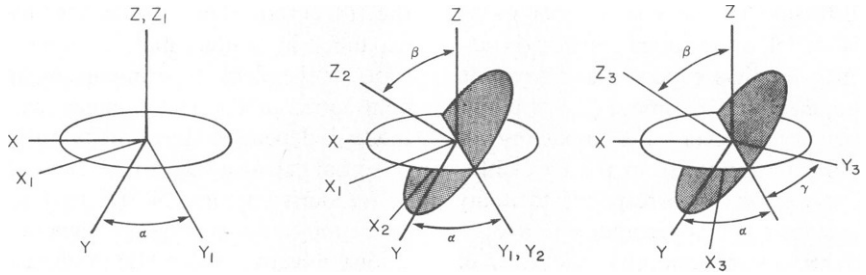

FIGURE 1 The Euler angles. Three successive rotations performed in sequence describe the orientation of a rigid body in space. First, a rotation about the z axis through angle α. Second, a rotation about the y_1 axis through angle β. Third a rotation about the z_2 axis through angle γ.

The matrix elements are calculated using the relations

$$L_1 D^{\ell}_{m,n} = \tfrac{1}{2}\{(\ell - n)(\ell + n + 1)\}^{1/2} D^{\ell}_{m,n+1} + \tfrac{1}{2}\{(\ell - n + 1)(\ell + n)\}^{1/2} D^{\ell}_{m,n-1} \quad (10a)$$

$$L_2 D^{\ell}_{m,n} = \frac{i}{2}\{(\ell - n)(\ell + n + 1)\}^{1/2} D^{\ell}_{m,n+1} - \frac{i}{2}\{(\ell - n + 1)(\ell + n)\}^{1/2} D^{\ell}_{m,n-1} \quad (10b)$$

$$L_3 D^{\ell}_{m,n} = n D^{\ell}_{m,n} \quad (10c)$$

$$D^{j_1}_{m_1,k_1} D^{j_2}_{m_2,k_2} = \sum_{j=|j_1-j_2|}^{j_1+j_2} (-1)^{m+k} (2j + 1) D^{j}_{m,k} \begin{pmatrix} j_1 & j_2 & j \\ m_1 & m_2 & -m \end{pmatrix} \begin{pmatrix} j_1 & j_2 & j \\ k_1 & k_2 & -k \end{pmatrix} \quad (10d)$$

and the orthogonality condition of Eq. 8. The quantity

$$\begin{pmatrix} j_1 & j_2 & j \\ m_1 & m_2 & -m \end{pmatrix}$$

is a Wigner 3-j symbol (24).

The matrix elements $\langle j', h', k' | H | j, h, k \rangle$ for a symmetric molecule such that $D_1 = D_2$ are explicitly,

$$\begin{aligned}
&\langle j', h', k' | H | j, h, k \rangle \\
&= [D_1 j(j + 1) + (D_3 - D_1)k^2]\, \delta_{j',j}\, \delta_{k',h}\, \delta_{k',k} \\
&\quad + \sum_{\substack{\ell,m \\ n}} f_{\ell,m,n}(-1)^{k+k'} \left(\frac{2\ell + 1}{8\pi^2}\right)^{1/2} (2j + 1)^{1/2}(2j' + 1)^{1/2} \\
&\quad \times [D_1 \ell(\ell + 1) + (D_3 - D_1)n^2] \times \begin{pmatrix} \ell & j & j' \\ m & h & -h' \end{pmatrix} \begin{pmatrix} \ell & j & j' \\ n & k & -k' \end{pmatrix} \\
&\quad - \sum_{\substack{\ell,m \\ n}} \sum_{\substack{\ell',m' \\ n'}} f_{\ell,m,n} f_{\ell',m',n'} (-1)^{h+k} \\
&\quad \times \left(\frac{2\ell + 1}{8\pi^2}\right)^{1/2} \left(\frac{2\ell' + 1}{8\pi^2}\right)^{1/2} \sum_{L} (2L + 1) \\
&\quad \times \begin{pmatrix} \ell & \ell' & L \\ m & m' & -M \end{pmatrix} \begin{pmatrix} L & j & j' \\ M & h & -h' \end{pmatrix} \begin{pmatrix} L & j & j' \\ N & k & -k' \end{pmatrix} \\
&\quad \times \left\{ D_1 [(\ell - n)(\ell + n + 1)\,(\ell' - n' + 1)(\ell' + n')]^{1/2} \right. \\
&\quad \times \begin{pmatrix} \ell & \ell' & L \\ n + 1 & n' - 1 & -N \end{pmatrix} \\
&\quad \left. + nn' D_3 \begin{pmatrix} \ell & \ell' & L \\ n & n' & -N \end{pmatrix} \right\}. \qquad (11)
\end{aligned}$$

Application to Time-resolved Fluorescence Anisotropy Decay

In a TRFAD experiment the polarized fluorescence intensity from fluorophores specifically attached to mobile elements of the biological assembly is observed. This intensity is the projection of $P(\Omega, t)$ onto $[\mathbf{v}(\chi) \cdot \mu_e]^2$, where $\mathbf{v}(\chi)$ is a unit vector in the direction of polarization along which the emitted light is observed, χ is its angle from the z axis, see Fig. 2; and μ_e is the unit electric dipole moment for emission of the fluorophore. $\mathbf{v}(\chi)$ is fixed in the lab frame and μ_e is fixed in the molecular frame (the frame fixed in the elemental subunit). It is convenient to express $\mathbf{v}$ and μ_e in a spherical basis using the transformations

$$\begin{aligned} V^1 &= -\sqrt{1/2}\,(V_x + iV_y) \qquad V^0 = V_z \\ V^{-1} &= \sqrt{1/2}\,(V_x - iV_y), \end{aligned} \quad (12)$$

where V_x, V_y, and V_z are cartesian components of a vector (24). We express $\mathbf{v}(\chi)$ in terms of the lab frame coordinates using the Wigner rotation matrix

$$V^{m}_{\text{mol}} = \sum_{m'} D^{1}_{m',m} V^{m'}_{\text{lab}} \quad (13)$$

and find

$$[\mathbf{v}(\chi) \cdot \mu_e]^2 = \sum_{\substack{m,m' \\ n,n'}} (-1)^{m+n} \mu_e^{-m} \mu_e^{-n} S^{m',n'} D^{1}_{m',m} D^{1}_{n',n} \quad (14)$$

where

$$\begin{aligned} S^{m',n'} &= K_a \mathbf{v}_1^{m'} \mathbf{v}_1^{n'} + [K_b \cos^2(\chi) + K_c \sin^2(\chi)] \mathbf{v}_2^{m'} \mathbf{v}_2^{n'} \\ &\quad + [K_b \sin^2(\chi) + K_c \cos^2(\chi)] \mathbf{v}_3^{m'} \mathbf{v}_3^{n'} \\ &\quad + 2(K_c - K_b) \sin(\chi) \cos(\chi) \mathbf{v}_2^{m'} \mathbf{v}_3^{n'}. \end{aligned} \quad (15)$$

Constants K_a, K_b, and K_c in Eq. 15 are related to the numerical aperture of the collection optics for emitted light polarized in the x, y, and z directions of the lab frame (19, 25). The unit vectors $\mathbf{v}_1$, $\mathbf{v}_2$, and $\mathbf{v}_3$ point along the x, y, and z axis in the lab frame. Finally, the observed fluorescence signal, F, is

$$F = F_0 \int_{\Omega_0} d\Omega\, P(\Omega, t)\, (\mathbf{v} \cdot \mu_e)^2, \quad (16)$$

where F_0 is a constant. As shown above $P(\Omega, t)$ is found from the solution to the Sturm-Liouville equation, $Q(\Omega, t)$, and the original substitution $P(\Omega, t) = P_0^{1/2} Q(\Omega, t)$. Using Eqs. 5 and 6 this is explicitly

$$P(\Omega, t) = \sum_i a_i \exp(-E_i t) \sum_{\substack{\ell,m \\ n}} q^{i}_{\ell,m,n} \times \left(\frac{2\ell + 1}{8\pi^2}\right)^{1/2} P_0^{1/2} D^{\ell}_{m,n}(\Omega). \quad (17)$$

For the calculation of the observed F from Eq. 16 it is desirable to have $P(\Omega, t)$ in the form

$$P(\Omega, t) = \sum_i a_i \exp(-E_i t) \sum_{\substack{\ell,m \\ n}} p^i_{\ell,m,n} \left(\frac{2\ell+1}{8\pi^2}\right)^{1/2} D^{\ell}_{m,n}(\Omega). \quad (18)$$

With the definition of $g^{\ell',m',n'}_{\ell,m,n}$ as

$$g^{\ell',m',n'}_{\ell,m,m} = \left(\frac{2\ell+1}{8\pi^2}\right)^{1/2} \int_{\Omega_0} d\Omega\, D^{*\ell}_{m,n}(\Omega)\, P_0^{1/2}(\Omega)\, D^{\ell'}_{m',n'}(\Omega) \quad (19)$$

that is calculable from P_0, we can show using Eq. 8 that Eqs. 18 and 19 require

$$p^i_{\ell,m,n} = \sum_{\substack{\ell',m' \\ n'}} q^i_{\ell',m',n'} \left(\frac{2\ell'+1}{8\pi^2}\right)^{1/2} g^{\ell',m',n'}_{\ell,m,n}. \quad (20)$$

Substituting the expanded version of $P(\Omega, t)$ from Eq. 18 and $(\mathbf{v} \cdot \mu_e)^2$ from Eq. 14 into Eq. 16 and performing the integration indicated using Eqs. 10d and 8 we find

$$\begin{aligned} F = F_0 \sum_i a_i \exp(-E_i t) \Bigg\{ & \frac{1}{3}(K_a + K_b + K_c)\sqrt{8\pi^2}\, p^i_{0,0,0} \\ & + \left(\frac{8\pi^2}{5}\right)^{1/2} \Bigg[S^{1,1} \Bigg\{ \mu_e^{-1}\mu_e^{-1}(p^i_{2,-2,-2} + p^i_{2,2,-2}) \\ & + \mu_e^{1}\mu_e^{1}(p^i_{2,-2,2} + p^i_{2,2,2}) + \sqrt{2}\mu_e^{0}\mu_e^{-1}(p^i_{2,-2,-1} \\ & + p^i_{2,2,-1}) + \sqrt{2}\mu_e^{0}\mu_e^{1}(p^i_{2,-2,1} + p^i_{2,2,1}) + \left(\frac{2}{3}\right)^{1/2}(\mu_e^{1}\mu_e^{-1} \\ & + \mu_e^{0}\mu_e^{0})(p^i_{2,-2,0} + p^i_{2,2,0}) \Bigg\} - \sqrt{1/2}\, S^{1,0} \Bigg\{ \mu_e^{-1}\mu_e^{-1} \\ & \times (p^i_{2,-1,-2} + p^i_{2,1,-2}) + \mu_e^{1}\mu_e^{1}(p^i_{2,-1,2} + p^i_{2,1,2}) \\ & + \sqrt{2}\mu_e^{0}\mu_e^{-1}(p^i_{2,-1,-1} + p^i_{2,1,-1}) + \sqrt{2}\,\mu_e^{0}\mu_e^{1}(p^i_{2,-1,1} \\ & + p^i_{2,1,1}) + \left(\frac{2}{3}\right)^{1/2}(\mu_e^{1}\mu_e^{-1} + \mu_e^{0}\mu_e^{0})(p^i_{2,-1,0} + p^i_{2,1,0}) \Bigg\} \\ & + \left(\frac{2}{3}\right)^{1/2}(S^{1,-1} + S^{0,0}) \Bigg\{ \mu_e^{-1}\mu_e^{-1} p^i_{2,0,-2} + \mu_e^{1}\mu_e^{1} p^i_{2,0,2} \\ & + \sqrt{2}\,\mu_e^{0}\mu_e^{-1} p^i_{2,0,-1} + \sqrt{2}\,\mu_e^{0}\mu_e^{1} p^i_{2,0,1} \\ & + \left(\frac{2}{3}\right)^{1/2}(\mu_e^{1}\mu_e^{-1} + \mu_e^{0}\mu_e^{0})\, p^i_{2,0,0} \Bigg\} \Bigg] \Bigg\}. \end{aligned} \quad (21)$$

We specify a_i from an initial condition on $Q(\Omega, t)$. For a TRFAD experiment

$$Q(\Omega, t=0) = P_0^{1/2}[\mathbf{E}(\epsilon) \cdot \mu_a]^2 = \sum_i a_i \varphi_i(\Omega), \quad (22)$$

where μ_a is the unit electric dipole moment for absorption, $\mathbf{E}(\epsilon)$ is the unit electric field vector of the excitation light, and ϵ is the angle $\mathbf{E}$ makes with the lab z axis, see Fig. 2.

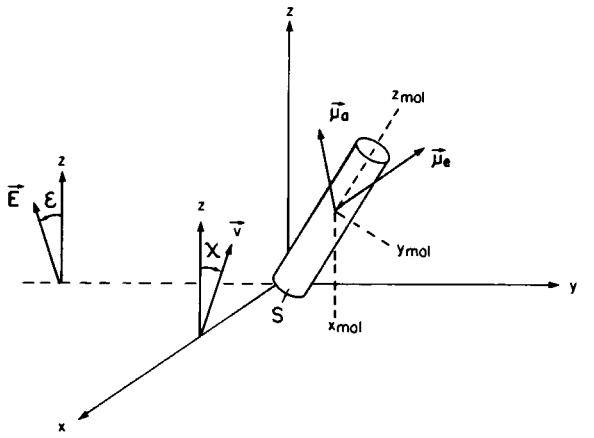

FIGURE 2 The geometry of the time-resolved fluorescence polarization experiment performed on an ordered system. A molecular coordinate frame defined by (x_{mol}, y_{mol}, z_{mol}) is fixed in a subunit, S, of the ordered assembly. The absorption and emission dipoles μ_a and μ_e are also fixed in this frame. Coordinates (x, y, z) define the laboratory frame. The excitation beam has a linearly polarized electric field vector $\mathbf{E}$ and propagates along the y axis. Vector $\mathbf{E}$ makes an angle ϵ with the z axis. Fluorescent emission is collected with optics positioned along the x axis. The polarization of the emission is analyzed along vector $\mathbf{v}$, which is in the yz plane and makes an angle χ with the z axis.

The eigenvectors $\varphi_i(\Omega)$ are orthonormal so we can invert Eq. 22 to solve for a_i. Using Eqs. 6 and 22 we find

$$a_i = \sum_{\substack{\ell,m \\ n}} q^{*i}_{\ell,m,n} \left(\frac{2\ell+1}{8\pi^2}\right)^{1/2} \times \int_{\Omega_0} d\Omega\, D^{*\ell}_{m,n}(\Omega)\, (\mathbf{E} \cdot \mu_a)^2\, P_0^{1/2}(\Omega). \quad (23)$$

Expressing $\mathbf{E}(\epsilon)$ and μ_a in a spherical basis using Eq. 12 and rotating $\mathbf{E}(\epsilon)$ into the molecular frame using Eq. 13 we find

$$(\mathbf{E} \cdot \mu_a)^2 = \sum_{\substack{m,m' \\ n,n'}} (-1)^{m+n} \mu_a^{-m} \mu_a^{-n} E^{m'} E^{n'} D^{1}_{m',m} D^{1}_{n',n}. \quad (24)$$

Eq. 23 can be integrated using Eqs. 19, 24, 10d, and 8 such that

$$\begin{aligned} a_i = \sum_{\substack{\ell,m,n \\ \ell',m',n'}} \sum_{\substack{h,h' \\ k,k'}} & (-1)^{h'+k'} q^{*i}_{\ell,m,n} \\ & g^{*\ell,m,n}_{\ell',m',n'} (2\ell+1)^{1/2}(2\ell'+1)^{1/2} \mu_a^{-h} \mu_a^{-k} \\ & \times E^{h} E^{k} \begin{pmatrix} 1 & 1 & \ell' \\ h' & k' & -m' \end{pmatrix} \begin{pmatrix} 1 & 1 & \ell' \\ h & k & -n' \end{pmatrix}. \end{aligned} \quad (25)$$

The coefficients $p^i_{\ell,m,n}$ in Eq. 18 are the amplitudes of the relaxation modes available to the system. The modes relax to the equilibrium configuration with relaxation time $1/E_i$. The magnitude of the $p^i_{\ell,m,n}$'s, calculated from Eq. 20, is related to the equilibrium angular distribution P_0. The relaxation modes that contribute to the TRFAD signal (only those with $\ell = 0, 2$) are identified in Eq. 21.

Application to the Restricted Rotational Diffusion of Cross-Bridges in a Relaxed Muscle Fiber

In a related paper (22) we apply the formalism of the previous sections to cross-bridges in a muscle fiber. For these measurements we employ low aperture excitation and collection optics so that **E** is linearly polarized and $K_a = K_b = 0$. If we assume P_0 depends only on the Euler angles β and γ (not α) and that the linearly polarized excitation light points along the lab z axis, then the polarization anisotropy, defined by the relation

$$r(t) \equiv \frac{F(\epsilon = 0, \chi = 0) - F(\epsilon = 0, \chi = 90°)}{F(\epsilon = 0, \chi = 0) + 2F(\epsilon = 0, \chi = 90°)} \tag{26}$$

is given by

$$r(t) = \frac{\left(\frac{3}{10}\right)^{1/2} \sum_i a_i \exp(-E_i t) \left\{ \mu_e^{-1}\mu_e^{-1} p^i_{2,0,-2} + \mu_e^1 \mu_e^1 p^i_{2,0,2} + \sqrt{2}(\mu_e^0 \mu_e^{-1} p^i_{2,0,-1} + \mu_e^0 \mu_e^1 p^i_{2,0,1}) + \left(\frac{2}{3}\right)^{1/2} (\mu_e^1 \mu_e^{-1} + \mu_e^0 \mu_e^0) p^i_{2,0,0} \right\}}{\sum_i a_i \exp(-E_i t) p^i_{0,0,0}}, \tag{27}$$

where

$$a_i = \sum_{\ell,m,n} p^{*i}_{\ell,0,m+n} \{8\pi^2(2\ell + 1)\}^{1/2} \mu_a^{-m} \mu_a^{-n} \begin{pmatrix} 1 & 1 & \ell \\ 0 & 0 & 0 \end{pmatrix} \begin{pmatrix} 1 & 1 & \ell' \\ m & n & -m-n \end{pmatrix} \tag{28}$$

and

$$p^{*i}_{\ell,0,n} = (2\ell + 1)^{1/2} \sum_{\ell',n'} (-1)^{n'} q^i_{\ell',0,n'} \left(\frac{2\ell' + 1}{4\pi}\right)^{1/2} \sum_j \times (2j + 1)^{1/2} \begin{pmatrix} \ell & \ell' & j \\ 0 & 0 & 0 \end{pmatrix} \begin{pmatrix} \ell & \ell' & j \\ -n & n' & n - n' \end{pmatrix} \times \int \sin(\beta) d\beta d\gamma \, P_0^{1/2} \, Y_{j,n'-n}(\beta, \gamma). \tag{29}$$

In Eq. 29 $Y_{\ell,m}$ is a spherical harmonic (26), and the domain of integration is $0 \le \beta \le \pi$, $0 \le \gamma \le 2\pi$. The denominator in Eq. 27 is time dependent, unlike the anisotropy for free rotational diffusion.

Approximation of the Equilibrium Angular Distribution from Fluorescent-labeled Muscle Fibers

The application of steady-state fluorescence polarization measurements to estimate P_0 is based on the assumption that the probe carrying molecule is acted on only by those torques that confine it in its local environment, and that a reference frame fixed in the local environment of the restricted molecule is a constant rotation from the laboratory fixed frame. The importance of this assumption is most easily demonstrated by an example of fluorescent-labeled lipids in vesicles dispursed in solution. In its local environment the lipid is confined in the membrane. Relative to a laboratory fixed frame, however, the lipid is randomly distributed and the vesicles themselves are freely rotationally diffusing and consequently applying nonlocal torques on the lipids. Steady-state measurements on this system would indicate their angular distribution to be random despite the local ordering of the lipids in the membrane.

The steady-state fluorescence polarization from relaxed muscle fibers indicate the fibers possess cylindrical symmetry about the fiber axis (27). We choose the fiber axis to correspond to the lab frame z axis in Fig. 2. This implies the cross-bridges are randomly oriented relative to the fiber axis, i.e., their angular distribution is independent of Euler angle α. However, because the cross-bridges project from the thick filament radially, a locally fixed frame is probably not a single rotation from the lab fixed frame so that P_0 is not necessarily independent of α. We do make the assumption that P_0 is independent of α but the assumption is based on evidence from TRFAD experiments performed on muscle fibers oriented nearly parallel to the excitation beam propagation direction. In these experiments, described in detail in a related paper (22), the anisotropy relaxation times are related to cross-bridge rotational motion about an axis parallel to the fiber axis. This relaxation time should be influenced by the α dependence of P_0. The data indicates the cross-bridge is moving relatively freely in this degree of freedom suggesting P_0 is independent of α.

The determination of P_0 as a function of the other degrees of freedom (corresponding to Euler angles β and γ) is correctly done by the steady-state measurements. The model-independent treatment of steady-state fluorescence polarization from extrinsic fluorescent probes in biological assemblies leads to a series of equations restricting the order parameters of the elements to which the probes are attached (18). Several workers have measured the steady-state fluorescence polarization from 5-[2-(iodoacetyl) aminoethyl] aminonapthalene-1-sulfonic acid (1,5-IAEDANS)-labeled muscle fibers (28–30). We use the model-independent equations with the data of Wilson and Mendelson, 1983 (referred to as WM) to approximate the angular distribution of cross-bridges in relaxed muscle fibers.[1]

[1]To accurately measure the steady-state angular distribution of the cross-bridges, the lifetime of the fluorescent probe should be much shorter than the rotational correlation time of the cross-bridge (18). Alternatively, in time-resolved measurements the probe lifetime should be long enough to detect the correlation time of the cross-bridge motion. Although the lifetime of the probe 1,5-IAEDANS is intermediate such that it can perform both tasks, other probes may not be so versatile. When the probe lifetime is long enough for the time-resolved measurements but

The general expression for the fluorescence polarization signal from a muscle fiber possessing cylindrical symmetry about the fiber axis is, in the present notation (from Eq. 16, reference 18)

$$\frac{F}{F_0} = \frac{1}{9}\sqrt{8\pi^2}\,p^0_{0,0,0} + \sum_{J=0}^{4}\sum_{k=-J}^{J} p^0_{J,0,k}\left(\frac{8\pi^2}{2J+1}\right)^{1/2} \times \left[\left(\frac{1}{3}z_0 m^a_k + \frac{1}{3}b_0 m^e_k\right)\delta_{J,2} + d^{J+}_0 M^J_k\right], \quad (30)$$

where $p^0_{J,0,k}$ are order parameters related to P_0 by Eq. 18 such that

$$P_0 \equiv P(\Omega, t \to \infty) = \sum_{\substack{\ell,m \\ n}} p^0_{\ell,m,n}\left(\frac{2\ell+1}{8\pi^2}\right)^{1/2} D^{\ell}_{m,n}(\Omega) \quad (31)$$

and

$$z_0 = \left(\frac{2}{3}\right)^{1/2}\left[\cos^2(\epsilon) - \frac{1}{2}\sin^2(\epsilon)\right]$$
$$b_0 = \left(\frac{2}{3}\right)^{1/2}\left[\cos^2(\chi) - \frac{1}{2}\sin^2(\chi)\right] \quad (32a)$$

$$d^{J+}_0 = -\frac{1}{4}[(-1)^J + 1]\sin^2(\epsilon)\sin^2(\chi)\,\langle 2,2,-2,2|J,0\rangle + \frac{2}{3}\left[\cos^2(\epsilon) - \frac{1}{2}\sin^2(\epsilon)\right]\left[\cos^2(\chi) - \frac{1}{2}\sin^2(\chi)\right] \times \langle 2,2,0,0|J,0\rangle + [(-1)^J - 1]\sin(\epsilon)\cos(\epsilon) \times \sin(\chi)\cos(\chi)\,\langle 2,2,1,-1|J,0\rangle \quad (32b)$$

$$M^J_0 = \mu^{-1}_a\mu^{-1}_a\mu^1_e\mu^1_e\langle 2,2,-2,2|J,0\rangle + \mu^1_a\mu^1_a\mu^{-1}_e\mu^{-1}_e\langle 2,2,2,-2|J,0\rangle + \mu^0_a\mu^{-1}_a\mu^0_e\mu^1_e 2\langle 2,2,-1,1|J,0\rangle + \mu^0_a\mu^1_a\mu^0_e\mu^{-1}_e 2\langle 2,2,1,-1|J,0\rangle + (\mu^1_a\mu^{-1}_a + \mu^0_a\mu^0_a)(\mu^1_e\mu^{-1}_e + \mu^0_e\mu^0_e) \times 2/3\langle 2,2,0,0|J,0\rangle \quad (32c)$$

$$M^J_{\pm 1} = \mu^0_a\mu^{\pm 1}_a\mu^{\pm 1}_e\mu^{\pm 1}_e\sqrt{2}\langle 2,2,\mp 2,\pm 1|J,\mp 1\rangle + \mu^{\pm 1}_a\mu^{\pm 1}_a\mu^0_e\mu^{\mp 1}_e\sqrt{2}\langle 2,2,\pm 1,\mp 2|J,\mp 1\rangle + \mu^0_a\mu^{\pm 1}_a(\mu^1_e\mu^{-1}_e + \mu^0_e\mu^0_e)\sqrt{4/3}\langle 2,2,0,\mp 1|J,\mp 1\rangle + (\mu^1_a\mu^{-1}_a + \mu^0_a\mu^0_a)\mu^0_e\mu^{\pm 1}_e\sqrt{4/3}\langle 2,2,\mp 1,0|J,\mp 1\rangle \quad (32d)$$

$$M^J_{\pm 2} = \mu^0_a\mu^{\pm 1}_a\mu^0_e\mu^{\pm 1}_e 2\langle 2,2,\mp 1,\mp 1|J,\mp 2\rangle + \mu^{\pm 1}_a\mu^{\pm 1}_a(\mu^1_e\mu^{-1}_e + \mu^0_e\mu^0_e)\sqrt{2/3}\langle 2,2,0,\mp 2|J,\mp 2\rangle + (\mu^1_a\mu^{-1}_a + \mu^0_a\mu^0_a)\mu^{\pm 1}_e\mu^{\pm 1}_e\sqrt{2/3}\langle 2,2,\mp 2,0|J,\mp 2\rangle \quad (32e)$$

$$M^J_{\pm 3} = \mu^0_a\mu^{\pm 1}_a\mu^{\pm 1}_e\mu^{\pm 1}_e\sqrt{2}\langle 2,2,\mp 2,\mp 1|J,\mp 3\rangle + \mu^{\pm 1}_a\mu^{\pm 1}_a\mu^0_e\mu^{\pm 1}_e\sqrt{2}\langle 2,2,\mp 1,\mp 2|J,\mp 3\rangle \quad (32f)$$

$$M^J_{\pm 4} = \mu^{\pm 1}_a\mu^{\pm 1}_a\mu^{\pm 1}_e\mu^{\pm 1}_e\langle 2,2,2,2|J,4\rangle \quad (32g)$$

$$m^{a,e}_0 = \sqrt{2/3}(\mu^1_{a,e}\mu^{-1}_{a,e} + \mu^0_{a,e}\mu^0_{a,e}) \quad (32h)$$

$$m^{a,e}_{\pm 1} = \sqrt{2}\mu^{\pm 1}_{a,e}\mu^0_{a,e} \quad (32i)$$

$$m^{a,e}_{\pm 2} = \mu^{\pm 1}_{a,e}\mu^{\pm 1}_{a,e}. \quad (32j)$$

The symbols $\langle j_1, j_2, k_1, k_2|j, k\rangle$ are Clebsch-Gordon coefficients (24). WM summarized their data with the three ratios $F_\parallel$, $F_\perp$, and $G_\parallel$ such that

$$F_\parallel \equiv \frac{F(\epsilon = 0, \chi = 0) - F(\epsilon = 0, \chi = 90°)}{F(\epsilon = 0, \chi = 0) + F(\epsilon = 0, \chi = 90°)} \quad (33a)$$

$$F_\perp \equiv \frac{F(\epsilon = 90°, \chi = 90°) - F(\epsilon = 90°, \chi = 0)}{F(\epsilon = 90°, \chi = 90°) + F(\epsilon = 90°, \chi = 0)} \quad (33b)$$

$$G_\parallel \equiv \frac{F(\epsilon = 0, \chi = 0) - F(\epsilon = 90°, \chi = 0)}{F(\epsilon = 0, \chi = 0) + F(\epsilon = 90°, \chi = 0)} \quad (33c)$$

Combining Eqs. 30 and 33 we obtain three equations restricting the values of $p^0_{J,0,k}$ such that

$$-\frac{2}{9}F_\parallel\sqrt{8\pi^2}\,p^0_{0,0,0} + \sum_{J,k} p^0_{J,0,k}\left(\frac{8\pi^2}{2J+1}\right)^{1/2}\left\{-\left(\frac{8}{27}\right)^{1/2}F_\parallel m^a_k\delta_{J,2} + \left(\frac{1}{6}\right)^{1/2}\left(1 - \frac{1}{3}F_\parallel\right)m^e_k\delta_{J,2} + \langle 2,2,0,0|J,0\rangle\left(1 - \frac{1}{3}F_\parallel\right)M^J_k\right\} = 0 \quad (34a)$$

$$-\frac{2}{9}F_\perp\sqrt{8\pi^2}\,p^0_{0,0,0} + \sum_{J,k} p^0_{J,0,k}\left(\frac{8\pi^2}{2J+1}\right)^{1/2}\left\{\left(\frac{2}{27}\right)^{1/2}F_\perp m^a_k\delta_{J,2} - \left(\frac{1}{6}\right)^{1/2}\left(1 + \frac{1}{3}F_\perp\right)m^e_k\delta_{J,2} + \frac{1}{2}\left[\langle 2,2,0,0|J,0\rangle\left(1 + \frac{1}{3}F_\perp\right) - \langle 2,2,-2,2|J,0\rangle(1 - F_\perp)\right]M^J_k\right\} = 0 \quad (34b)$$

$$-\frac{2}{9}G_\parallel\sqrt{8\pi^2}\,p^0_{0,0,0} + \sum_{J,k} p^0_{J,0,k}\left(\frac{8\pi^2}{2J+1}\right)^{1/2}\left\{\left(\frac{1}{6}\right)^{1/2}\left(1 - \frac{1}{3}G_\parallel\right)m^a_k\delta_{J,2} - \left(\frac{8}{27}\right)^{1/2}G_\parallel m^e_k\delta_{J,2} + \langle 2,2,0,0|J,0\rangle\left(1 - \frac{1}{3}G_\parallel\right)M^J_k\right\} = 0. \quad (34c)$$

For the three Eqs. 34a–c and one more equation from the normalization of P_0 there are 15 unknown order parameters. There are no further restrictions on these

too long for the steady-state measurement, in some cases one can reduce the lifetime of the probe for the steady-state measurements by adding a fluorescence quencher (31).

parameters implied from steady-state fluorescence polarization data using 1,5-IAEDANS as the probe. Under these circumstances we can only make plausible simplifying, model-dependent assumptions about the angular arrangement of the cross-bridges in the muscle fiber to reduce the degrees of freedom in Eq. 34.

Mirror reflection symmetry such that any one half-sarcomere has a mirror reflection in the opposite half-sarcomere is sometimes assumed for muscle fibers (32). Imposing this requirement on P_0 requires $p^0_{J,0,k} = 0$ when $J = 1$ or 3. Furthermore, the cross-bridges in a relaxed fiber are known to be rather highly disordered from ESR studies (33). This observation has led investigators to presume that γ dependence in P_0 is absent (28, 34). We use this observation to justify neglecting the highest order γ related order parameters such that $p^0_{4,0,\pm 2} = p^0_{4,0,\pm 4} = 0$. Finally, for the orientations of μ_a and μ_e that are experimentally justified (see the next paragraph) we must require, $p^0_{2,0,-1} = p^0_{2,0,1} = 0$ and $p^0_{2,0,2} = p^0_{2,0,-2}$ so that the degrees of freedom in the order parameters of Eqs. 34 are reduced to four. Thus, with Eqs. 34 and the normalization of P_0 we can solve for $p^0_{0,0,0}$, $p^0_{2,0,0}$, $p^0_{2,0,2}$, and $p^0_{4,0,0}$.

Up to now we have assumed the quantities m^a_k, m^e_k, and M_k, that depend on the direction of the absorption and emission dipole moments μ_a and μ_e in Eqs. 32c–j, are known. Previously, TRFAD measurements performed on the head portion of the myosin molecule (subfragment 1 or S-1) that is labeled with 1,5-IAEDANS and bulk dissolved have given some indication of the orientation of the probe relative to the hydrodynamic principal axis frame of the protein fragment (3). From these studies it is indicated that if

$$\mu_a = [\sin(\theta_a)\cos(\phi_a), \sin(\theta_a)\sin(\phi_a), \cos(\theta_a)]$$
$$\mu_e = [\sin(\theta_e)\cos(\phi_e), \sin(\theta_e)\sin(\phi_e), \cos(\theta_e)] \quad (35)$$

and the hydrodynamic principal frame (our molecular frame) has its z axis along the long dimension of the ellipsoid of revolution shape given to S-1, then θ_a and θ_e are $<40°$ and $\phi_a = \phi_e = 0$. At excitation and emission wavelengths that differ from those employed in reference 3, WM found that the angle between the absorption and emission dipole is 18° and that $35° < \theta_a < 45°$ and $18° < \theta_e < 36°$ is consistent with their data when a Gaussian distribution of cross-bridges in the relaxed muscle fiber is assumed. When $\theta_a = 40°$ and $\theta_e = 22°$ is assumed and with Eqs. 32, 34, and 35 we now suggest that

$$P_0(\beta,\gamma) = 0.045\,Y_{0,0} + 0.0239\,Y_{2,0}(\beta,\gamma) + 0.000798[Y_{2,-2}(\beta,\gamma) + Y_{2,2}(\beta,\gamma)] + 0.00797\,Y_{4,0}(\beta,\gamma) \quad (36)$$

represents a reasonable approximation to P_0 in relaxed muscle fibers. Other choices for θ_a and θ_e consistent with the constraints mentioned above do not qualitatively alter this angular distribution. Given this P_0 Eqs. 27–29 have two free parameters, the rotational diffusion constants D_1 and D_3, to determine the observed time course of the anisotropy $r(t)$. We vary D_1 and D_3 to best fit the experimental anisotropy curves from labeled cross-bridges in muscle fibers. These experiments are described in detail in a related paper (22). When $D_1 = 1.25 \times 10^5\ s^{-1}$ and $D_3 = 3.0 \times 10^5\ s^{-1}$ we find

$$r(t) = 0.04 + 0.03\exp(-t/1{,}585\ \text{ns}) + 0.20\exp(-t/1{,}000\ \text{ns}) + \text{negligible terms}, \quad (37)$$

which is well approximated by $r(t) = 0.25\exp(-t/1{,}000$ ns) as measured for the relaxed muscle fiber data (22).

Time-resolved Fluorescence Polarization Signals from Fibers in Other Geometries

We have presented the formal solution to the problem of rotational diffusion in a general three-dimensional angular potential. However, in the application of the two previous sections we have assumed the angular potential is independent of one of these dimensions. We have further argued that this assumption is appropriate for the relaxed muscle fiber when its symmetry (fiber) axis points along the direction of polarization of the excitation light (the vertical fiber geometry). When the fiber is oriented in any other direction this assumption is not necessarily valid. We performed TRFAD experiments on fibers when the fiber axis is positioned at 90° to the excitation light polarization (the horizontal fiber geometry) (22). We wish to use the theory to make an approximate calculation of the anisotropy relaxation time for the horizontal fiber to determine if the theory can anticipate the observed result.

If we approximate the angular potential of the vertical fiber to lowest order, only terms proportional to $f_{2,0,0}$ in the potential remain (see Eq. 7). In this approximation the angular potential depends only on the Euler angle β (see Fig. 1). When the fiber axis is rotated

$$f'_{\ell,m,n} = \sum_k f_{\ell,k,n}\, D^{\ell *}_{k,m}(\alpha_0,\beta_0,\gamma_0), \quad (38)$$

where $f'_{\ell,m,n}$ are the order parameters describing the potential in the rotated frame and α_0, β_0, and γ_0 are the Euler angles of the coordinate rotation. When the fiber is rotated by 90° such that the fiber axis is perpendicular to the excitation light polarization and at 45° to the beam propagation direction (the experimental horizontal fiber geometry), $\alpha_0 = -\pi/4$, $\beta_0 = \pi/2$, and $\gamma_0 = 0$. Then $f'_{2,0,0} = -f_{2,0,0}/2$, $f'_{2,-2,0} = i\sqrt{6}/4\, f_{2,0,0}$, and $f'_{2,2,0} = -i\sqrt{6}/4\, f_{2,0,0}$. Ignoring $f'_{2,-2,0}$ and $f'_{2,2,0}$ and applying the calculation of the two previous sections using $f'_{2,0,0}$ in place of $f_{2,0,0}$ we find the anisotropy relaxation time of the horizontal fiber to be $\sim 2/3$ that of the vertical fiber. Our observation of the anisotropy relaxation time of the horizontal fiber to

be ~350 ns compared with ~1,000 ns for the vertical fiber confirms the trend anticipated by the above calculation.

METHODS

Symbolic algebraic manipulation was performed using a symbolic manipulation program (SMP) (Inference Corp., Pasadena, CA) installed on a VAX 750 virtual memory computer (Digital Equipment Corp., Marlboro, MA). Explicit symbolic calculation and numerical evaluation of Eqs. 11 and 26–29, and the diagonalization and calculation of eigenvectors of the matrix in Eq. 11 were performed on SMP. An error in SMP's evaluation of some of the Wigner 3-j symbols was corrected by an independent program for this evaluation. The programs used in this calculation for use in SMP are available from the author.

Diagonalization and calculation of eigenvectors of the matrix of Eq. 11 were performed for the specific application described in theory. For this application the matrix, **H**, with elements $\langle j', 0, k'|H|j, 0, k\rangle$ was diagonalized. It can be shown from Eq. 11 and the symmetry properties of the Wigner 3-j symbols (24) that these matrix elements are zero unless $j' + j$ and $k' + k$ equal even integers. This property implies **H** can be diagonalized for even j, j', k, and k' independently from odd j, j', k, and k'. It can be shown from Eqs. 27 and 29 that only eigenvectors of H that include even j contribute to the TRFAD signal. Thus, diagonalization of **H** for even j, j', k, and k' is all that is required for the calculation of the anisotropy decay curve.

We performed the diagonalization of **H** for the two cases when, $j, j' \leq 4$ and $j, j' \leq 6$. The relaxation times, $1/E_i$, and amplitudes, $p^l_{i,m,n}$, are identical in those two calculations for those relaxation times and amplitudes that contribute to the anisotropy relaxation curves for relaxed vertical fibers, i.e., $i = 0, 1, 2$ in Eq. 27 (see Eq. 37). This result indicates that the approximation of the infinite matrix **H** with elements terminating at $j = j' = 4$ is sufficient for the angular potential found in the relaxed muscle fibers.

DISCUSSION

The theory describes an approach to the problem of rotational diffusion in a potential that is very generally applicable to biological assemblies. Our theory is used here with the time-resolved fluorescence polarization technique. A new feature of this treatment is that it adopts the previously introduced model-independent approach to describe the angular potential that restricts rotational diffusion and incorporates the information of the time-independent measurements into the time-dependent calculation. We have also applied the calculation to the motion of myosin cross-bridges in relaxed muscle fibers that have the fluorescent probe 1,5-IAEDANS specifically attached to the cross-bridge. The results of these studies are described in detail in a related publication (22).

The analytical methods of this approach are fundamentally quite similar to the earlier work for ESR probes in lipid membranes (35–36). Other treatments of time-resolved fluorescence polarization from elements in restricted rotational diffusion lack the generality of the present treatment in that they impose restrictions on the functional dependence of the potential and/or the mathematical form of the potential is assumed a priori (8, 15, 37). The present treatment avoids these problems by allowing the potential to be arbitrary and subject only to the requirement that it can be described as an expansion in a complete set of orthonormal functions. The utility of this approach is demonstrated on a real biological system in another publication (22).

The author thanks N. L. Thompson for helpful suggestions, M. F. Morales, and L. Peller for critically reading this manuscript, H. Martinez for assistance in using the VAX computer, and J. Junkin for help in typing this manuscript.

This work was supported by a Postdoctoral Fellowship from the American Heart Association (reference number 82 071), AHA Grant CI-8, and by Public Health Service grant HL-16683.

Received for publication 28 January 1985 and in final form 29 May 1985.

REFERENCES

1. Ehrenberg, M., and R. Rigler. 1972. Polarized fluorescence and rotational Brownian motion. *Chem. Phys. Lett.* 14:539–544.
2. Chuang, T. J., and K. B. Eisenthal. 1972. Theory of fluorescence depolarization by anisotropic rotational diffusion. *J. Chem. Phys.* 57:5094–5097.
3. Mendelson, R. A., M. F. Morales, and J. Botts. 1973. Segmental flexibility of the S-1 moiety of myosin. *Biochemistry.* 12:2250–2255.
4. Yguerabide, J., H. F. Epstein, and L. Stryer. 1970. Segmental flexibility in an antibody molecule. *J. Mol. Biol.* 51:573–590.
5. Torgerson, P. M. 1984. Tryptophan emission from myosin subfragment 1: acrylamide and nucleotide effect monitored by decay-associated spectra. *Biochemistry.* 23:3002–3007.
6. Badea, M., and L. Brand. 1979. Time-resolved fluorescence measurements. *Methods Enzymol.* 61:378–425.
7. Mendelson, R. A., and P. H. Cheung. 1976. Muscle crossbridges: absence of direct effect of calcium on movement away from the thick filaments. *Science (Wash. DC).* 194:190–192.
8. Kinosita, K., S. Kawato, and A. Ikegami. 1977. A theory of fluorescence polarization decay in membranes. *Biophys. J.* 20:289–305.
9. Lipari, G., and A. Szabo. 1980. Effect of librational motions on fluorescence depolarization and nuclear magnetic resonance relaxation in macromolecules and membranes. *Biophys. J.* 30:489–506.
10. Heyn, M. D. 1979. Determination of lipid order parameters and rotational correlation times from fluorescence depolarization experiments. *FEBS (Fed. Eur. Biochem. Soc.) Lett.* 108:359–364.
11. Jahnig, F. 1979. Structural order of lipids and proteins in membranes: evaluation of fluorescence anisotropy data. *Proc. Natl. Acad. Sci.* USA. 76:6361–6365.
12. Kawato, S., K. Kinosita, and A. Ikegami. 1978. Effect of cholesterol on the molecular motion in the hydrocarbon region of lecithin bilayers studied by nanosecond fluorescence techniques. *Biochemistry.* 17:5026–5031.
13. Favro, L. D. 1960. Theory of rotational Brownian motion of a free rigid body. *Phys. Rev.* 119:53–62.
14. Polnaszek, C. F., G. V. Bruno, and J. H. Freed. 1973. ESR line shapes in the slow-motional region: anisotropic liquids. *J. Chem. Phys.* 58:3185–3199.
15. Szabo, A. 1980. Theory of polarized fluorescent emission in uniaxial liquid crystals. *J. Chem. Phys.* 72:4620–4626.
16. Mendelson, R. A., and P. H. Cheung. 1978. Intrinsic segmental flexibility of the S-1 moiety of myosin using single-headed myosin. *Biochemistry.* 17:2139–2148.
17. Chandrasekhar, S. 1943. Stochastic problems in physics and astronomy. *Rev. Mod. Phys.* 15:1–89.
18. Burghardt, T. P. 1984. Model-independent fluorescence polarization for measuring order in a biological assembly. *Biopolymers.* 23:2383–2406.
19. Burghardt, T. P., and N. L. Thompson. 1984. Effect of planar

dielectric interfaces on fluorescence emission and detection: Evanescent excitation with high-aperture collection. *Biophys. J.* 46:729–738.
20. Thompson, N. L., H. M. McConnell, and T. P. Burghardt. 1984. Order in supported phospholipid monolayers detected by the dichroism of fluorescence excited with polarized evanescent illumination. *Biophys. J.* 46:739–748.
21. Burghardt, T. P., and N. L. Thompson. 1985. Model-independent electron spin resonance for measuring order of slowly moving components in a biological assembly. *Biophys. J.* 48:401–409.
22. Burghardt, T. P., and N. L. Thompson. 1985. Motion of myosin cross-bridges in skeletal muscle fibers studied by time-resolved fluorescence anisotropy decay. *Biochemistry.* 24:3731–3735.
23. Landau, L. D., and E. M. Lifshitz. 1959. Fluid Mechanics. Pergamon Press, Elmsford, NY. 219–229.
24. Davydov, A. S. 1963. Quantum Mechanics. NEO Press, Ann Arbor, MI. 127–169.
25. Axelrod, D. 1979. Carbocyanine dye orientation in red cell membrane studied by microscopic fluorescence polarization. *Biophys. J.* 26:557–573.
26. Arfken, G. 1970. Mathematical Methods for Physicists. Academic Press, Inc., New York. 569–574.
27. Burghardt, T. P., T. Ando, and J. Borejdo. 1983. Evidence of cross-bridge order in contraction of glycerinated skeletal muscle. *Proc. Natl. Acad. Sci.* USA. 80:7515–7519.
28. Wilson, M. G. A., and R. A. Mendelson. 1983. A comparison of order and orientation of crossbridges in rigor and relaxed muscle fibres using fluorescence polarization. *J. Muscle Res. Cell Motil.* 4:671–693.
29. Borejdo, J., and S. Putnam. 1977. Polarization of fluorescence from single skinned glycerinated rabbit psoas fibers in rigor and relaxation. *Biochim. Biophys. Acta.* 459:578–595.
30. Borejdo, J., O. Assulin, T. Ando, and S. Putnam. 1982. Cross-bridge orientation in skeletal muscle measured by linear dichroism of an extrinsic chromophore. *J. Mol. Biol.* 158:391–414.
31. Cantor, C. R., and P. R. Schimmel. 1980. Biophysical Chemistry. Part II: Techniques for the Study of Biological Structure and Function. Freeman Publications, San Francisco. 447.
32. Morales, M. F. 1984. Calculation of the polarized fluorescence from a labeled muscle fiber. *Proc. Natl. Acad. Sci. USA.* 81:145–149.
33. Thomas, D. D., and R. Cooke, 1980. Orientation of spin labeled myosin heads in glycerinated muscle fibers. *Biophys. J.* 32:891–906.
34. Mendelson, R. A., and M. G. A. Wilson, 1982. Three-dimensional disorder of dipolar probes in a helical array. Application to muscle cross-bridges. *Biophys. J.* 39:221–227.
35. Polnaszek, C. F., and J. H. Freed. 1975. Electron spin resonance studies of anisotropic ordering, spin relaxation, and slow tumbling in liquid crystalline solvents. *J. Phys. Chem.* 79:2283–2306.
36. Nordio, P. L., G. Rigatti, and U. Segre. 1972. Spin relaxation in nematic solvents. *J. Chem. Phys.* 56:2117–2123.
37. Zannoni, C., A. Arcioni, and P. Cavatorta. 1983. Fluorescence depolarization in liquid crystals and membrane bilayers. *Chem. Phys. Lipids.* 32:179–250.